

Research article

**ACCUMULATION OF AQUAPORIN-1 DURING HEMOLYSIN-INDUCED NECROTIC CELL DEATH**KELLY SCHWEITZER<sup>1</sup>, ERRAN LI<sup>2</sup>, VENKATARAMANA SIDHAYE<sup>1</sup>, VIRGINIA LEITCH<sup>1</sup>, SERGEY KUZNETSOV<sup>1</sup> and LANDON S. KING<sup>1\*</sup><sup>1</sup>Department of Medicine, Division of Pulmonary and Critical Care Medicine Johns Hopkins University School of Medicine, 5501 Hopkins Bayview Circle Baltimore, MD 21224, USA, <sup>2</sup>Institute of Respiratory Disease, China Medical University, Shenyang, China

**Abstract:** Altered tissue water homeostasis may contribute to edema formation during various stresses including bacterial infection. We observed induction of aquaporin-1 (AQP1) during *Staphylococcus aureus* infection of cultured cells indicating a potential mechanism underlying altered water homeostasis during infection. To investigate mechanisms of AQP1 induction, we examined the effects of the *S. aureus*  $\alpha$ -hemolysin on AQP1 abundance in Balb/c fibroblasts. Fibroblasts incubated with 30  $\mu$ g/ml hemolysin exhibited a 5-10 fold increase in AQP1 protein within 4-6 hours of exposure. The use of multiple signaling cascade inhibitors failed to affect hemolysin-mediated accumulation of AQP1. However, immunoprecipitation revealed an initial accumulation of ubiquitinated AQP1 followed by a decrease to baseline levels after 4 hours. Immunofluorescence indicated that following hemolysin exposure, AQP1 was no longer on the plasma membrane, but was found in a population of sub-membrane vacuoles. AQP1 redistribution was further indicated by surface biotinylation experiments suggesting diminished AQP1 abundance on the plasma membrane as well as redistribution out of lipid raft fractions. Live cell confocal microscopy revealed that the pattern of cell volume change observed following hemolysin exposure was altered in cells in which AQP1 was silenced.

---

\*Author for correspondence; e-mail: [lsking@jhmi.edu](mailto:lsking@jhmi.edu), tel: 443-287-3347, fax: 410-287-3349

Abbreviations used: AQP – aquaporin; MAPK – mitogen-activated protein kinase; siRNA – small interfering RNA

We conclude that alpha-toxin alters proteasomal processing and leads to intracellular accumulation of AQP1, which may likely contribute to disrupted cell volume homeostasis in infection.

**Key words:** Aquaporin, Toxin, Ubiquitin, Lipid raft

## INTRODUCTION

Aquaporins (AQPs) are a family of membrane channels that are in general highly permeable to water [1]. To date, thirteen mammalian aquaporin homologues (AQP0-AQP12) have been identified, and aquaporins are present at all levels of life [2]. The evolutionary conservation of aquaporins suggests mediation of water homeostasis under wide-ranging environmental conditions. First identified in 1992 [3], aquaporin-1 (AQP1) is expressed at numerous sites including vascular endothelium, renal proximal tubule epithelium, biliary epithelium, and choroid plexus [2]. Studies of both mice and humans have determined that AQP1 plays a fundamental role in urinary concentration, as well as pulmonary vascular permeability [4-6]. More recently, AQP1 has also been shown to participate in cell migration and angiogenesis [7].

Changes in tissue water homeostasis are a known consequence of bacterial infection, generally manifest as local or systemic edema. Mechanisms underlying disrupted water homeostasis are not fully defined. In this study we describe increased AQP1 abundance in response to *S. aureus*  $\alpha$ -hemolysin (alpha-toxin). Proteasomal activity markedly decreases following alpha toxin exposure coincident with an increase in abundance of AQP1 and redistribution of AQP1 from the plasma membrane to intracellular vacuoles following exposure. Dysregulation of AQP1 in response to the *S. aureus* alpha-toxin may contribute to changes in cell volume regulation, and provide insights into potential mechanisms by which bacterial toxins disrupt cell and tissue water homeostasis.

## MATERIALS AND METHODS

### Drugs, chemicals, antibodies

PD98059 (50  $\mu$ M), SB203580 (30  $\mu$ M), and SP600125 (30  $\mu$ M) were obtained through Calbiochem (San Diego, CA). Other drugs used were obtained from Calbiochem unless otherwise specified. Staurosporin (4  $\mu$ M) was purchased from Sigma-Aldrich (St. Louis, MO). Anti-ubiquitin antibodies were purchased from Santa-Cruz (Santa Cruz, CA). Antibodies to AQP1 were from Alpha Diagnostics. HRP-conjugated antibodies to the beta subunit of cholera toxin (GM-1) and anti- $\beta$ -actin were obtained from Sigma-Aldrich (St. Louis, MO). Anti-mouse and anti-rabbit HRP-conjugated secondary antibodies were obtained through Amersham (Piscataway, NJ). Inhibitors targeting distinct signaling pathways previously implicated in either AQP regulation or alpha toxin response were also assayed for their ability to suppress the AQP1 induction including

JNK (SAPK inhibitor 1, whose mode of action is distinct from SP600125, 30  $\mu$ M), caspases (Caspase Inhibitor VI, 5  $\mu$ M), protein kinase C (R0-31-8425, 10  $\mu$ M), Rho (Y27632, 5  $\mu$ M), MLCK (SM-1, 50 nM), Phospholipase C (U73122), and farnesyl-transferase (FTI-277, 10  $\mu$ M). These inhibitors failed to suppress the observed induction of AQP1 caused by alpha-toxin treatment.

### **Cell culture**

Standard cell culture techniques were employed throughout this study. Balb/c fibroblasts were obtained from ATCC and were cultured in 5% CO<sub>2</sub> as described previously [9]. These cells have been successfully used by our lab to study AQP1 and no other aquaporin is expressed using RT-PCR or by immunoblot. Unless otherwise stated, cells were incubated for 5 hours with 30  $\mu$ g/ml alpha toxin in standard medium lacking serum or antibiotics. As indicated, cells were pre-treated for 45min with drugs or inhibitors listed above.

### **Immunoblotting**

Standard SDS-PAGE was performed as described [9, 26]. Following treatment as described, cells were lysed in RIPA buffer (50 mM Tris pH 7.5, 0.1% SDS, 0.5% Na deoxycholate, 1% NP-40, 150 mM NaCl) with Complete Protease Inhibitor cocktail (Roche; Indianapolis, IN) and incubated on ice for 30 minutes. Total protein was determined using the bicinchoninic acid (BCA) assay (Pierce; Rockford, IL).

Five to fifteen micrograms protein per sample was resolved on 12.5% SDS-PAGE gels, transferred to PVDF, and incubated with the designated antibodies. Immunoblots were visualized using ECL-Plus (Amersham; Piscataway, NJ) or SuperSignal (Pierce; Rockford, IL).

### **Cell death assessment**

*LDH release.* Membrane integrity was assayed using CytoTox-ONE Homogenous Membrane Integrity Assay (Promega; Madison, WI) following manufacturers specifications. LDH release was recorded as relative fluorescence units with excitation and emission wavelengths of 560 nM and 590 nM, respectively.

*Caspase activity.* Caspase 3/7 activity was determined using Caspase-Glo 3/7 Assay (Promega; Madison, WI) and expressed as relative luminescence units after one hour. Caspase-Glo 8 and Caspase-Glo 9 Assays (Promega; Madison, WI) were utilized to determine Caspase 8 and 9 activities. To measure caspase cleavage, Balb/c fibroblasts were either untreated or treated with 500 nM staurosporin or 35  $\mu$ g/ml alpha toxin. Protein was purified and resolved on SDS-PAGE using general methods. Immunoblots were probed for AQP1 and caspase 3 cleavage.

*Cell viability.* Cell viability was determined using the CellTiter Glo Assay (Promega; Madison, WI) measuring ATP production compared to controls. ATP concentration was recorded as relative luminescence units.

*DNA fragmentation.* DNA fragmentation was analyzed based on the generation of mono- and oligonucleosomes during apoptotic cell death. Presence of mono- and oligonucleosomes was quantified using the Cell Death Detection ELISA-Plus (Roche; Indianapolis, IN) at A490 nM.

### **Immunoprecipitation**

AQP1 immunoprecipitations were performed as previously described [9]. At the indicated time points following alpha toxin exposure, cells were lysed in Solubilization Buffer (20 mM Tris (pH 8.0), 200 mM NaCl, 1% (v/v) Triton X-100, 1% (w/v) deoxycholate, 0.1% (w/v) SDS, 5 mM EDTA, 5 mM EGTA, Complete Protease Inhibitor cocktail tablet). N-ethylmaleimide (5 mM) and 1 µg/ml ubiquitin aldehyde were added to the Solubilization Buffer to limit deubiquitination. The lysate was precleared by incubation with 50% Protein A-Sepharose (Sigma; St. Louis, MO) slurry, centrifuged (3,000 x g; 2 min; 4°C), and then incubated with 1 µg of rabbit IgG (Sigma; St. Louis, MO) or polyclonal AQP1 at 4°C. Protein A-Sepharose, previously blocked with 10% (w/v) BSA, was added and the lysate incubated at 4°C overnight. The immunoprecipitated samples were recovered following centrifugation (3,000 x g; 2 min; 4°C), washed four times for 5 min each with Solubilization Buffer, then washed once for 5 min with Salt-free Wash Buffer (20 mM Tris (pH 8.0), 1% (v/v) Triton X-100, 5 mM EDTA, 5 mM EGTA). Immunoprecipitated proteins were eluted from the Sepharose by incubation in Elution Buffer (10 mM Tris (pH 6.8), 3% (w/v) SDS, 10% (v/v) glycerol, 0.01% (w/v) bromophenol blue and 0.5 M dithiothreitol) for 30 min at 37°C. The eluted proteins were subjected to SDS-PAGE as described above.

### **Real time quantitative PCR**

Real time quantitative PCR (RT-qPCR) was performed in select experiments to quantify AQP1 and MSS1 mRNA abundance (Online Supplementary Data). Following exposures as noted, total RNA was isolated and assessed spectrophotometrically. Real Time primers were designed using Beacon Designer Software: AQP1 sense, 5'-GCTTGTCTGTGGCCCTTGG-3'; AQP1 antisense, 5'-AAGTTGCGGGTGAGCACAG-3'; MSS1, sense: 5'-ATGTTGGTGGCTGTAAAGG-3', antisense: 5'-AAGCATCAGTCCGATTGG-3'; 18S rRNA sense, 5'-CGGCTACCACATCCAAGGAA; 18S rRNA antisense, 5'-GCTGGAATTACCGCGGCT-3'. Primers were obtained from Applied Biosystems (Foster City, CA) or Integrated DNA Technologies (Coralville, IA). RT-qPCR reactions were assembled for iScript One Step RT-PCR for SYBR Green (Bio-Rad; Hercules, CA) following the manufacturers specifications and utilizing the Bio-Rad iCycler Thermal Cycler (Hercules, CA) with the following conditions: 50°C for 10 min, 95°C for 5 min, and 45 cycles at 95°C for 10 sec and 61.9°C for 30 sec. Relative changes in cycle threshold (.CT) values were calculated to determine mRNA expression. AQP1 mRNA was calculated as the fold change using the 2-ddCT method [27], and normalized to the CT values for 18S ribosomal mRNA using the Bio-Rad iCycler Data Analysis software.

**Proteasomal activity assays**

Cells were lysed in proteasomal activity lysis buffer (20 mM Tris pH 7.4, 0.1 mM EDTA, 20% glycerol (v/v), 0.04% NP-40, 1 mM  $\beta$ -mercaptoethanol, 5 mM ATP) and incubated on ice for 30 minutes. To quantify proteasomal activity, cell lysates (10-50  $\mu$ g) were added to 1 x proteasomal assay buffer (10 x stock: 250 mM HEPES pH 7.5, 5 mM EDTA, 0.5% NP-40, 0.02% SDS) and incubated with substrates (50-100  $\mu$ M) (Boc-LLG-bNAP, Suc-LLVY-AMC, or Boc-LRR-AMC; available from Biomol; Plymouth Meeting, PA). Fluorescence was measured at excitation and emission wavelengths of 398 nm and 490 nm, respectively.

**AQP1 protein redistribution studies**

*Confocal microscopy.* Balb/c fibroblasts were cultured on 4-well chamber slides, washed with PBS, and fixed using 4% formaldehyde, as previously described [26]. Visualization was performed using Alexa448-coupled rabbit IgG secondary antibodies. Images were acquired using the Noran Oz Confocal Laser Scanning Microscope System utilizing Intervision Software (ver6.5) on a silicon Graphics O2 platform.

*Surface biotinylation.* Surface biotinylation experiments were performed as previously described [26]. In brief, Balb/c fibroblasts were incubated with 0.5mg/ml Sulfo-NHS-LC-Biotin (Pierce; Rockford, IL) for 30 min at 4°C. To quench the reaction, cells were then washed with 50 mM Tris pH 8.0 in PBS pH 8.0. Cells were scraped into solubilization buffer (20 mM Tris pH 8.0, 200 mM NaCl, 1% Triton X-100, 1% deoxycholate, 0.1% SDS, 5 mM EDTA, Complete protease inhibitor cocktail). The supernatant was mixed with 1/5 volume ImmunoPure Immobilized streptavidin (Pierce; Rockford, IL) and incubated overnight at 4°C. Protein was eluted using 50  $\mu$ l 1 x Laemmli Buffer at 37°C for 30 min and resolved using SDS-PAGE.

*Sucrose density-gradient ultracentrifugation.* Cultured Balb/c fibroblasts were grown in three 100 mM dishes and treated using 30  $\mu$ g/ml alpha toxin for 5 hours for sucrose density gradient ultracentrifugation as described [28]. Cells were harvested and resolved using sucrose density gradient ultracentrifugation as previously described [28]. In brief, Balb/c fibroblasts were scraped into 2 ml sodium carbonate, pH 11.0. Cells were homogenized using a Polytron tissue grinder (three 10 sec bursts) followed by sonication (three 20 sec bursts). A 90% sucrose solution prepared in MBS (25 mM MES, pH 6.5, 0.15 M NaCl) was added to a final concentration of 45% and placed into an ultracentrifuge tube. A 5-35% discontinuous sucrose gradient was formed and centrifuged at 39,000 rpm for 24 h. Fractions (1 ml) were collected and resolved on SDS-PAGE and transferred to PVDF for immunoblotting.

**Cell volume measurements**

*siRNA knockdown of AQP1.* Balb/c fibroblasts were grown on chambered coverglass (Nunc) and transfected using 125 nM siRNA to mAQP1

(Dharmacon) or scramble siRNA control using GenePorter 2 transfection reagent following manufacturer's specifications. AQP1 silencing was confirmed by protein immunoblot.

*Relative cell volume measurements.* Relative cell size measurements have previously been used in the study of AQP1 function [29]. Here, we used confocal microscopy to determine relative cell volume. Balb/c fibroblasts or Balb/c cells with diminished AQP1 (using siRNA described above) were grown on chambered coverglass (Nunc) with 5  $\mu$ l of Image-IT (wheat germ agglutinin conjugated to Alexa Fluor 594, Molecular Probes) in 500  $\mu$ l of PBS, and incubated for 10 minutes at 37°C in each well, and excited at 594 nm wavelength to obtain optical sections. A time-lapsed series of 0.2 micron z-plane sections were scanned using an Ultraview 2 (Perkin-Elmer) confocal microscope using the 100 x magnification over 1 hour. 3-D reconstructions were created by merging single XY slices in a Z-series projection (Velocity 3). Cell boundaries were identified by manually localizing intensity of fluorescence, and volume calculations are performed using Velocity 3. Three cells per high-powered field were measured and the average volume calculated, and cell volumes in stimulated conditions are compared to control volumes. Untreated control cells were compared to cells treated with 30  $\mu$ g/ml of alpha-toxin at 1 minute, 5 minutes, 30 minutes and 60 minutes.

## RESULTS

### ***S. aureus* and alpha-hemolysin increase AQP1 abundance**

Bacterial infection is known to disrupt tissue water homeostasis. To examine the effect of the gram-positive bacterium *S. aureus* on AQP1 abundance in cultured cells, fibroblasts were incubated with live *S. aureus* at 37°C, and harvested at intervals to determine AQP1 abundance by immunoblotting (Fig. 1A). *S. aureus* produced an increase in AQP1 abundance evident as early as 4 hours after exposure. To assess the potential contribution of bacterial products to this induction, we tested the effects of the cell wall component lipotechoic acid (LTA) and the *S. aureus* toxin, alpha-hemolysin (alpha-toxin) on AQP1 abundance. LTA produced minimal and variable effects on AQP1 abundance (data not shown). In contrast,  $\alpha$ -toxin caused a dose-dependent and time-dependent increase in AQP1 protein (Fig. 1B). The increase in AQP1 was evident within 2 hours and maximal at a dose of 20  $\mu$ g/ml after 6 hours.

We have observed mitogen activated protein kinase (MAPK) dependent induction of AQP1 in osmotic stress (King, unpublished data) as others have reported [8]. To determine if MAPK activation is required for the increase in AQP1 abundance, Balb/c fibroblasts were treated with  $\alpha$ -toxin in the presence of MAPK inhibitors, PD98059 (ERK1/2), SB203580 (p38), and SP600125 (JNK1-3) (Fig. 2A). MAPK inhibitors failed to suppress the observed increase in AQP1 protein indicating that the upregulation of AQP1 was MAPK independent.

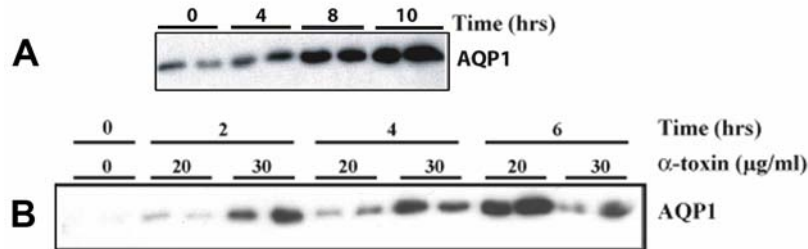


Fig. 1. *S. aureus* and alpha-hemolysin increase AQP1 abundance. A – Balb/c fibroblasts incubated with *Staphylococcus aureus* for intervals and immunoblots probed for AQP1. B – Balb/c fibroblasts were treated with alpha toxin for 2-6 hr and immunoblots of cell lysates were probed for AQP1.

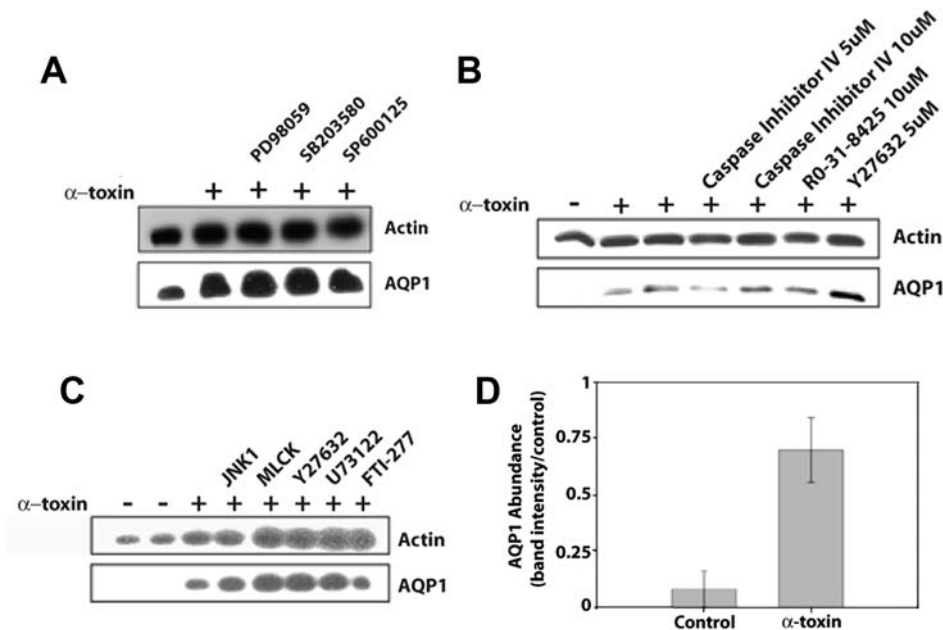


Fig. 2. MAPK-independent induction of AQP1. A – Balb/c fibroblasts were treated with 30 µg/ml of alpha toxin for 5 hr in the presence of MAPK inhibitors, ERK1/2 (PD998059; 50 µM), p38 (SB203580; 30 µM), and JNK (SP600125; 30 µM). B – Fibroblasts were treated with toxin in the presence of caspase inhibitors (5-10 µM), PKC (R0-31-8425; 10 µM), and Rho kinase (Y27632; 5 µM) inhibitors. C – Fibroblasts treated with toxin in the presence of the following inhibitors, JNK (SAPK inh I, 30 µM); MLCK (MLCK inhibitor peptide; 50 nM); Rho kinase (Y27632; 5 µM), PLC (U73122; 5 µM), and farnesyl-transferase (FTI-277; 10 µM). D – Densitometric analysis of AQP1 protein abundance (relative to actin controls) in untreated fibroblasts compared to alpha-toxin treated fibroblasts (n = 5).

Additional inhibitors targeting distinct signaling pathways previously implicated in either AQP regulation or alpha toxin response were also assayed for their ability to suppress the AQP1 induction including JNK (SAPK inhibitor 1, whose mode of action is distinct from SP600125, 30  $\mu$ M), Caspase Inhibitor VI (5  $\mu$ M), PKC (R0-31-8425, 10  $\mu$ M), Rho (Y27632, 5  $\mu$ M), MLCK (SM-1, 50 nM), PLC (U73122), and farnesyl-transferase (FTI-277, 10  $\mu$ M). These inhibitors failed to suppress the observed induction of AQP1 caused by  $\alpha$ -toxin treatment (Fig. 2B-C).

The induction of AQP1 in response to  $\alpha$ -toxin was highly reproducible with an average induction that was 6 x that of baseline AQP1 levels (Fig. 2D). In addition, RT-qPCR revealed that AQP1 gene expression did not change following alpha toxin exposure (Fig. 3), indicating the possibility of a post-translational mechanism underlying the increase in AQP1 abundance.

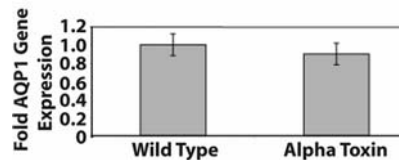


Fig. 3. AQP1 gene expression unaltered by alpha toxin. AQP1 gene expression was measured using Real-Time quantitative RT-PCR using SYBR-Green (Methods). Cells were untreated or treated with 30  $\mu$ g/ml alpha toxin for 5 hours and RNA was isolated for RT-qPCR.

#### Increase in ubiquitinated AQP1 following alpha toxin exposure

Our lab has previously shown that AQP1 is ubiquitinated, and protein degradation occurs via proteasomes rather than lysosomes [9]. To determine the contribution of ubiquitination and proteasomal activity to AQP1 accumulation following alpha-toxin, Balb/c fibroblasts were treated with 30  $\mu$ g/ml alpha toxin, AQP1 was immunoprecipitated, and immunoblots were probed with ubiquitin-specific antibodies. AQP1 ubiquitination markedly increased following 1 hr of alpha toxin exposure compared to the untreated controls (Fig. 4). Ubiquitination then decreased to near baseline levels at 4 hr of exposure.

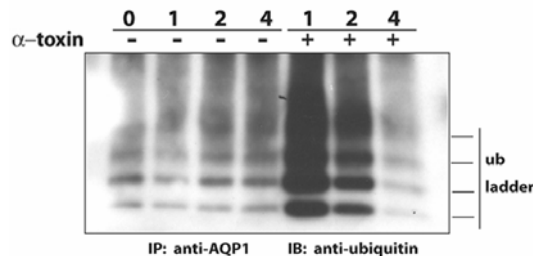


Fig. 4. AQP1 accumulates in ubiquitinated form. Balb/c fibroblasts were treated with 30  $\mu$ g/ml alpha toxin and AQP1 immunoprecipitated using 1  $\mu$ g rAQP1 antibody. Immunoprecipitated proteins were then blotted to PVDF and probed using ubiquitin antibodies to detect the classical ubiquitin ladder by western blot.

Proteasomal-mediated degradation of target proteins is ATP-dependent. Since ATP levels decreased in Balb/c fibroblasts following alpha-toxin (see below), we investigated whether proteasomal activity also decreased. Three proteasomal substrates were utilized to quantify proteasomal activity in cell lysates following alpha toxin exposure. As shown in Fig. 5A-C, proteasomal cleavage of 3 distinct substrates falls nearly to baseline activity following alpha toxin treatment.

Proteasomal activity may be regulated at least in part by changes in transcription of distinct proteasomal components following bacterial infection [10]. Consistent with this, RT-qPCR revealed that the relative gene expression for MSS1 [11, 12] decreased following alpha toxin exposure (normalized to total 18S). The change in relative gene expression correlates to a 1.6-fold change in total MSS1 gene expression following alpha toxin exposure (data not shown). These experiments indicate that alpha toxin causes accumulation of ubiquitinated AQP1 due to a significant decrease in proteasomal activity.

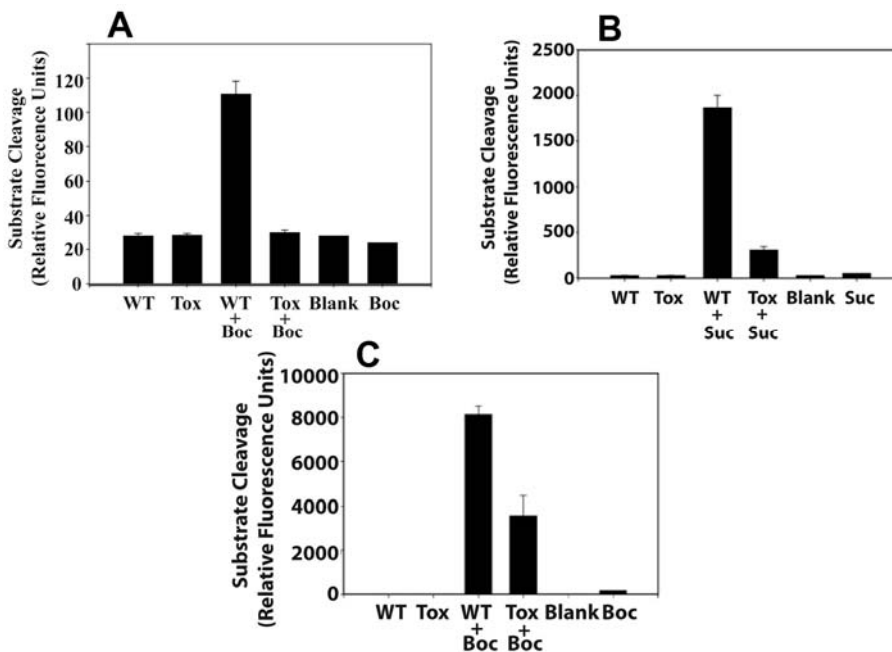


Fig. 5. Alpha toxin leads to proteasomal inhibition in Balb/c fibroblasts. Balb/c cells were treated with 30  $\mu\text{g/ml}$  alpha toxin and cell lysates were isolated. To quantify proteasomal activity, cell lysates (10-50  $\mu\text{g}$ ) were added to 1 x proteasomal assay buffer (10 x stock: 250 mM HEPES pH 7.5, 5 mM EDTA, 0.5% NP-40, 0.02% SDS) and incubated with substrates (50-100  $\mu\text{M}$ ) (Boc-LLG-bNAP, Suc-LLVY-AMC, or Boc-LRR-AMC) and incubated for 3 hr. From left to right, samples were either WT untreated, toxin treated, WT untreated in the presence of proteasomal substrate, toxin treated in the presence of proteasomal substrate, blank, and proteasomal substrate alone. The blank is without lysates or substrate. Substrate alone lacks lysates. A – Boc-LLG-NAP. B – Suc-LLVY-AMC. C – Boc-LRR-AMC. Fluorescence was measured at 490 nM.

### AQP1 distribution is altered by alpha toxin

To investigate potential effects of alpha toxin on AQP1 distribution, we used confocal immunofluorescence microscopy. Untreated fibroblasts exhibit distinct labeling of the cell membrane, as well as scattered intracellular labeling (Fig. 6A-C). Following 2.5 hours of alpha toxin exposure, AQP1 membrane labeling is markedly reduced, and small membrane blebs were observed. After 4 hours of alpha toxin, little AQP1 was detected on the plasma membrane and, labeling of peri-nuclear vacuoles was prominent.

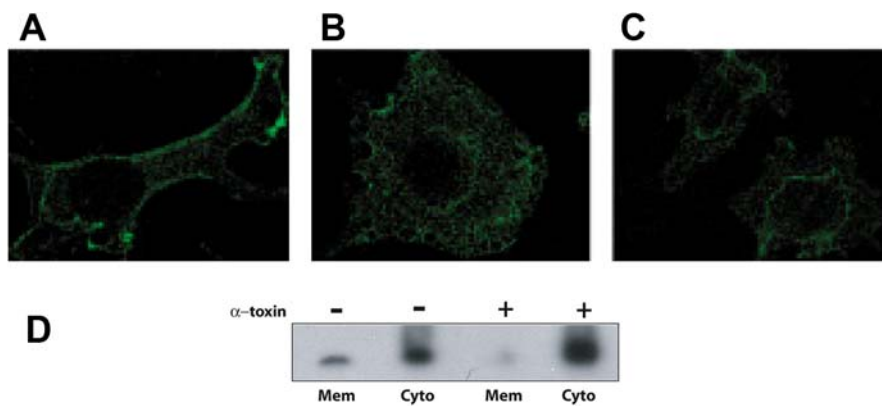


Fig. 6. AQP1 Internalization. Immunofluorescence confocal microscopy of AQP1 in untreated and alpha toxin treated Balb/c fibroblasts. A – Wild type. B – 2.5 hr exposure. C – 4 hr exposure. D – Surface biotinylation of membrane proteins and cytoplasmic and membrane proteins detected by immunoblots for AQP1.

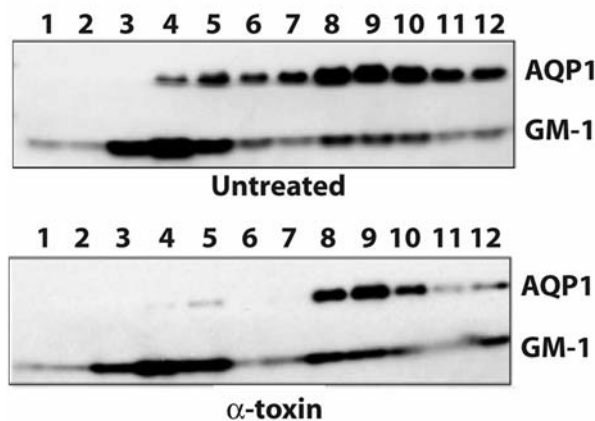


Fig. 7. AQP1 dissociates from lipid rafts. Sucrose density gradient ultracentrifugation was performed on cell lysates to isolate lipid raft fractions and AQP1 was detected by western blot. Cholera toxin B (GM-1) was used as a control for lipid rafts.

To confirm this redistribution, Balb/c fibroblasts were either untreated or treated with 30  $\mu\text{g}/\text{ml}$  alpha toxin for 5 hours, biotin was added to label membrane proteins, and cells were washed and lysed. Immunoprecipitation with streptavidin was performed on cell lysates to pull-down biotinylated proteins. Biotinylated AQP1 decreased after alpha toxin, while the fraction not bound by biotin increased (Fig. 6D). This result is consistent with the immunofluorescence data that indicate increased intracellular AQP1 following alpha toxin exposure.

AQP3, AQP5, AQP8 and AQP9 have been described to reside within cholesterol-rich microdomains on plasma membranes called lipid rafts [13-15]. The distribution of these rafts is highly cell-type specific and partitioning of AQP1 into lipid rafts has not been reported. We isolated lipid raft fractions using sucrose density gradient ultracentrifugation, and performed immunoblots to determine the partitioning of AQP1 into the fractions (Fig. 7). Consistent with previous reports describing other aquaporins in lipid rafts AQP1 resides in both lipid raft and non-lipid raft fractions. AQP1 is present in low-density fractions 4-5 where it partitions with GM-1, a recognized lipid raft marker, located in fractions 3-5. Following alpha toxin exposure, AQP1 is enriched within fractions 8-10, while GM-1 distribution was unchanged. In order to quantify changes in AQP1 partitioning, we used two different methods. First, we compared the ratio of AQP1 in low-density fractions (3-5) to high-density fractions (8-10) in control and alpha toxin treated samples. Using this method of comparison, we observed a 32% reduction in the ratio of AQP1 abundance in low-density lipid raft fractions (3-5) to high-density fractions (8-10). Secondly, we normalized to total GM1 and compared AQP1 abundance in low-density lipid raft fractions (3-5) compared to high-density fractions (8-10) in control and alpha toxin treated samples. Using this method of comparison, we observed an 81% and 84% reduction of total AQP1 abundance in low-density fractions 4 and 5, respectively. Data obtained by these two methods of analysis indicate that AQP1 is enriched within lipid raft fractions in un-stimulated Balb/c fibroblasts, and that alpha toxin stimulates redistribution into non-lipid raft membrane fractions. These data are consistent with the confocal and surface biotinylation experiments, which also indicate the redistribution of AQP1 in response to alpha toxin.

#### **Alpha toxin causes necrotic cell death in Balb/c fibroblasts**

It was evident from visual inspection that  $\alpha$ -toxin was toxic to cultured fibroblasts (also seen with live *S. aureus*). To characterize the cell death caused by alpha toxin exposure, we analyzed several markers. First, cell viability was determined by measuring ATP production. Untreated wild type cells continue to produce ATP for at least five hours (Fig. 8A). In contrast, ATP production decreased below baseline levels after one hour of exposure to 30  $\mu\text{g}/\text{ml}$  alpha toxin, consistent with necrotic cell death. Because caspase activation is a common precursor to apoptosis, we assayed caspase 3/7 activities. Cells were treated with 30  $\mu\text{g}/\text{ml}$  alpha toxin for 5 hours and caspase activity was measured.

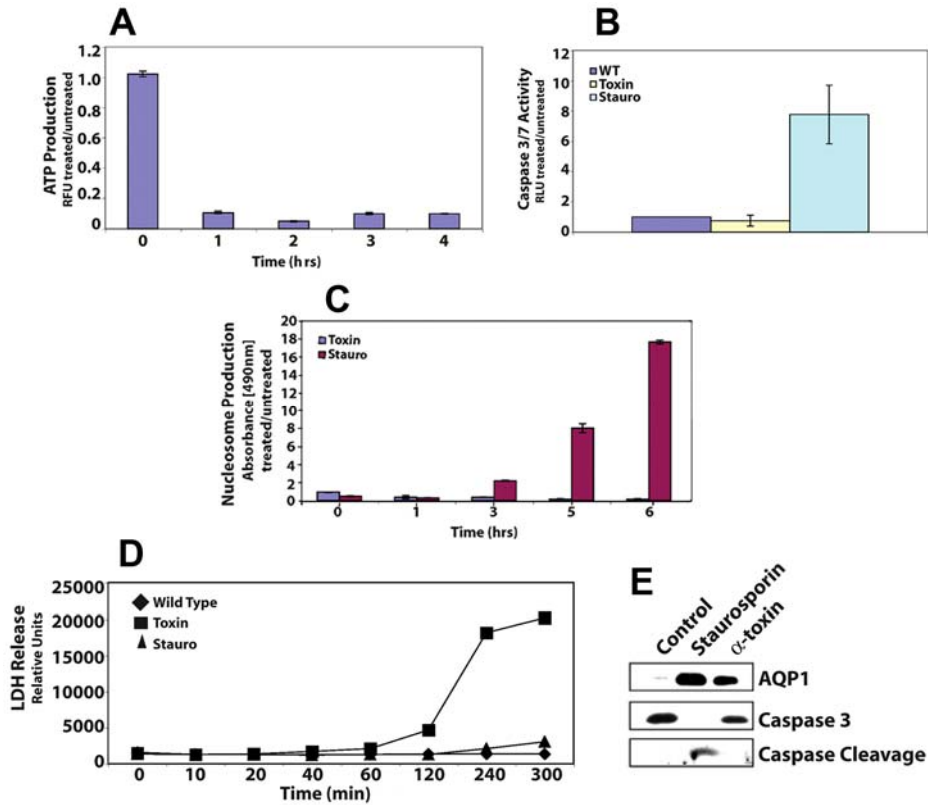


Fig. 8. Alpha toxin causes necrotic cell death in Balb/c fibroblasts. Cultured cells were treated with 30  $\mu$ g/ml alpha-toxin and harvested at the designated intervals to assess cell death by measuring. A – ATP production. B – Caspase 3/7 activity. C – Nucleosome production. D – LDH release. E – Immunoblot of Caspase 3 cleavage.

Caspase 3/7 activities were not different in untreated vs. treated cells (Fig. 8B), while the staurosporin (4  $\mu$ M) control produced clear caspase 3/7 activation. In addition protein immunoblots failed to show caspase cleavage following alpha toxin treatment (Fig. 8E). DNA fragmentation was quantified by oligonucleosome production following alpha toxin treatment (Fig. 8C). Oligonucleosome formation was observed with the staurosporin control, but DNA fragmentation was not observed in either untreated cells or in cells treated with  $\alpha$ -toxin. LDH release increased 1-2 hours following alpha toxin exposure and continued to increase for 5 hours (Fig. 8D). These data indicate that alpha toxin causes widespread necrotic cell death in Balb/c fibroblasts.

#### Alpha-toxin produces cell volume changes in fibroblasts

Relative cell volume changes in response to alpha toxin were analyzed using confocal microscopy of live cells. Fibroblasts grown on coverslips were transfected with control siRNA or the anti-AQP1 siRNA, and exposed to alpha

toxin. Reduction of AQP1 in siRNA treated cells was confirmed by immunoblot (Fig. 9A). Cell volume was determined at designated times (Fig. 9B). Within 5 minutes of exposure to alpha toxin, cell volume began to decrease in control-transfected cells, and continued to decrease out to 60 min (Fig. 9B). Cells in which AQP1 was reduced exhibited a markedly different volume response. Following alpha toxin exposure, cell volume increased, and continued to increase out to 60 min. Studies assessing apoptosis were repeated in the control and AQP1-siRNA treated cells. Silencing of AQP1 did not alter the pattern of cell death from that described above.

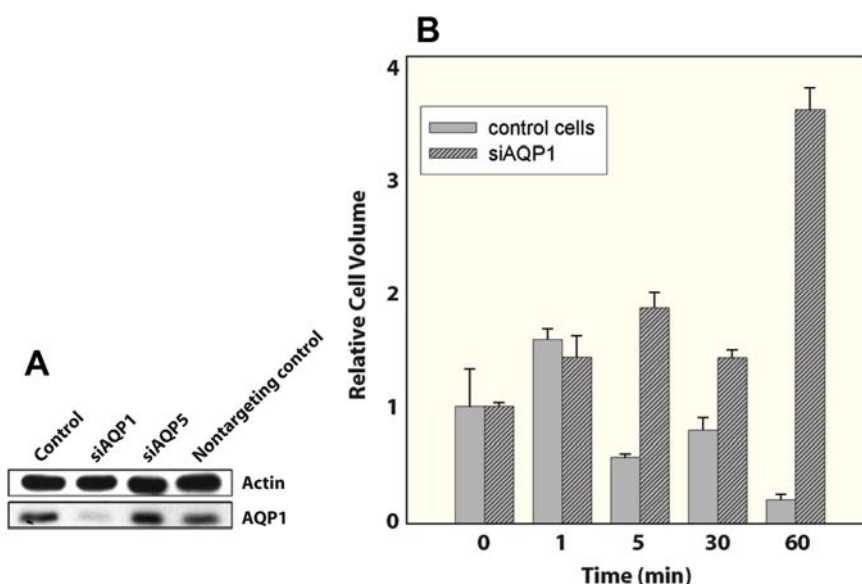


Fig. 9. Volume changes dependent on AQP1. A – AQP1 was silenced using AQP1-siRNA and detected by immunoblot. B – Balb/c fibroblasts were grown on glass coverslips with and without AQP1-siRNA, treated with 30  $\mu$ g/ml alpha-toxin, and cell volume was measured at time intervals using confocal microscopy.

## DISCUSSION

It is well recognized in clinical practice that bacterial infection alters local tissue fluid homeostasis, most commonly manifest as edema in the affected tissue. Beyond local effects, systemic release of bacterial toxins can produce cardiovascular instability and altered organ function, including disrupted water homeostasis and edema formation. While the consequences of infection are partially ascribed to the generation of pro-inflammatory cytokines and chemokines by the host that themselves produce pathophysiologic changes, bacterial products may directly alter cell function, and contribute to disruptions in water homeostasis.

These studies derived from the serendipitous observation of AQP1 induction by bacterial contamination of cultured fibroblasts. Here we describe that AQP1 abundance is increased by the *S. aureus* toxin alpha-hemolysin, or alpha-toxin. This increase in abundance occurs as a result of decreased activity of the proteasome and consequent decrease in ubiquitinated AQP1, rather than as a result of an increase in transcriptional activation of AQP1. More detailed investigation revealed an initial increase in ubiquitinated AQP1 followed by a marked decrease in ubiquitinated AQP1 that returned to near baseline levels. Similarly, we previously described that hypertonic induction of AQP1 resulted in part from decreased ubiquitination of the protein. Regulation of proteasomal subunit activity by bacterial infection has previously been reported, however this is the first example of alterations in abundance of a membrane transport protein as a result of changes in proteasome activity caused by a bacterial toxin.

This dynamic response does not only include a change in AQP1 abundance, but includes an alpha-toxin-stimulated redistribution of AQP1 from the cell membrane to a vacuolar compartment within the cell. This observation is consistent with a recent report that the bacterial pathogen *Citrobacter rodentium* disrupts normal plasma membrane localization of both AQP2 and AQP3 in colonocytes [16]. However, in contrast to the response to *S. aureus* and alpha toxin described in our study, *C. rodentium* did not alter AQP protein abundance. This redistribution off of the plasma membrane following alpha toxin stimulation, evident by immunofluorescence and biotinylation studies, occurred in parallel with a change in the lipid partitioning of AQP1 from low-density lipid-raft fractions to higher-density, non-raft fractions. At this point we do not know if the difference in lipid partitioning is an active component of the mechanism for the internalization of AQP1, or simply reflects the redistribution into an intracellular compartment. Given the increasingly well-established role for lipid rafts as a scaffold on which protein-protein interactions are organized, redistribution from raft fractions may prove relevant to the internalization [17]. However, the increase in ubiquitination prior to the change in AQP1 localization introduces the possibility that ubiquitin modification of AQP1 may contribute to its subsequent internalization. This increase in modification occurs prior to ATP depletion and dramatically decreases as ATP in the cell becomes exhausted suggesting that intracellular ATP concentrations, affected by necrotic cell death, could lead to a pathway regulating the ubiquitin-mediated internalization of channels rather than degradation.

A recent report describes mechanisms leading transcriptional regulation of cholesterol biosynthetic genes following exposure of cells to the pore-forming toxins aerolysin and *S. aureus*  $\alpha$ -toxin [18]. In these studies, bacterial toxin produces pores that facilitated K<sup>+</sup> efflux and subsequent caspase-1 activation, which was the upstream activator of sterol regulatory element binding protein (SREBP) and SREBP-responsive gene activation. In our studies, a general caspase inhibitor did not suppress the increase in AQP1 abundance in response to alpha toxin. Studies are underway to examine potential changes in ion channel

homeostasis caused by bacterial pore formation or bacterial infection to determine if these directly influence aquaporin expression.

We embarked on this project primarily to study mechanisms leading to the up-regulation of AQP1 abundance in response to bacterial infection, which has been consistently reproducible in our laboratory following challenge with a variety of bacterial species. We extended upon these initial experiments to determine the mechanism for this induction and to our surprise found that the hemolysin produced by *S. aureus* caused a similar increase in AQP1 abundance. This was an unexpected finding and a curious result in a cell with such damage to the plasma membrane. None-the-less, the consistency of the response to both bacterial infection and *S. aureus* alpha toxin made it overwhelmingly apparent that, although unexpected, the increase in AQP1 was a critical component in the response of Balb/c fibroblasts to such insults and could potentially contribute to the response of these cells to the changes in cell volume in response to such insults.

Changes in cell volume have been described in all forms of cell death [19-21]. In particular, cell shrinkage has been well described in apoptotic cell death [22-25]. In our studies, biochemical assessment indicated that necrotic cell death occurs downstream of alpha toxin exposure. The pattern of cell volume changes we observed followed by shrinkage is curious in light of the biochemical evidence pointing to necrosis. Unexpectedly, we found that silencing AQP1 produced a marked change in the volume response to alpha toxin that was highly reproducible. However, silencing AQP1 did not produce an apparent change in measured parameters of cell death in these studies, as we had expected. Therefore, at this time the physiologic consequence of this markedly altered cell volume response remains unclear. Although cells with diminished AQP1 have no significant change in relative cell volume, a stimulus (in this case alpha toxin) is required to initiate water movement through the aquaporin. Still, the dramatic alteration in cell volume response with silenced AQP1 revealed that AQP1 indeed contributes to maintaining water homeostasis even in cells with such plasma membrane damage. Although silencing AQP1 failed to alter the eventual cell death due to necrosis, altering cellular water permeability could contribute to a recovery program initiated by Balb/c fibroblasts following insult with bacterial infection or alpha toxin. Ongoing experiments will determine the physiologic significance of changes in AQP1 on the cell volume response in Balb/c fibroblasts.

In summary, *S. aureus* alpha toxin produced necrotic cell death in parallel with the internalization of AQP1 as well as an increase in its abundance resulting from decreased proteasomal activity. These observations provide new insight into potential mechanisms by which bacterial toxins may alter the function of membrane transport proteins, and thereby contribute to changes in water homeostasis in cells and tissues.

**Acknowledgements.** This work was supported by NHLB R01 HL 70217 and a Grant-in-Aid from the American Heart Association.

## REFERENCES

1. Preston, G.M. and Agre, P. Isolation of the cDNA for erythrocyte integral membrane protein of 28 kilodaltons: member of an ancient channel family. **Proc. Natl. Acad. Sci. U.S.A.** 88 (1991) 11110-11114.
2. King, L.S., Kozono, D. and Agre, P. From structure to disease: the evolving tale of aquaporin biology. **Nat. Rev. Mol. Cell. Biol.** 5 (2004) 687-698.
3. Preston, G.M., Carroll, T.P., Guggino, W.B. and Agre, P. Appearance of water channels in *Xenopus* oocytes expressing red cell CHIP28 protein. **Science** 256 (1992) 385-387.
4. King, L.S., Nielsen, S., Agre, P. and Brown, R.H. Decreased pulmonary vascular permeability in aquaporin-1-null humans. **Proc. Natl. Acad. Sci. U.S.A.** 99 (2002) 1059-1063.
5. Ma, T., Yang, B., Gillespie, A., Carlson, E.J., Epstein, C.J. and Verkman, A.S. Severely impaired urinary concentrating ability in transgenic mice lacking aquaporin-1 water channels. **J. Biol. Chem.** 273 (1998) 4296-4299.
6. King, L.S., Choi, M., Fernandez, P.C., Cartron, J.P. and Agre, P. Defective urinary-concentrating ability due to a complete deficiency of aquaporin-1. **N. Engl. J. Med.** 345 (2001) 175-179.
7. Saadoun, S., Papadopoulos, M.C., Hara-Chikuma, M. and Verkman, A.S. Impairment of angiogenesis and cell migration by targeted aquaporin-1 gene disruption. **Nature** 434 (2005) 786-792.
8. Umenishi, F. and Schrier, R.W. Hypertonicity-induced aquaporin-1 (AQP1) expression is mediated by the activation of MAPK pathways and hypertonicity-responsive element in the AQP1 gene. **J. Biol. Chem.** 278 (2003) 15765-15770.
9. Leitch, V., Agre, P. and King, L.S. Altered ubiquitination and stability of aquaporin-1 in hypertonic stress. **Proc. Natl. Acad. Sci. U.S.A.** 98 (2001) 2894-2898.
10. Schwan, W.R. and Kopecko, D.J. Uptake of pathogenic intracellular bacteria into human and murine macrophages downregulates the eukaryotic 26S protease complex ATPase gene. **Infect. Immun.** 65 (1997) 4754-4760.
11. Dubiel, W., Ferrell, K. and Rechsteiner, M. Peptide sequencing identifies MSS1, a modulator of HIV Tat-mediated transactivation, as subunit 7 of the 26 S protease. **FEBS Lett.** 323 (1993) 276-278.
12. Shibuya, H., Irie, K., Ninomiya-Tsuji, J., Goebel, M., Taniguchi, T. and Matsumoto, K. New human gene encoding a positive modulator of HIV Tat-mediated transactivation. **Nature** 357 (1992) 700-702.
13. Ishikawa, Y., Yuan, Z., Inoue, N., Skowronski, M.T., Nakae, Y., Shono, M., Cho, G., Yasui, M., Agre, P. and Nielsen, S. Identification of AQP5 in lipid rafts and its translocation to apical membranes by activation of M3 mAChRs in interlobular ducts of rat parotid gland. **Am. J. Physiol. Cell Physiol.** 289 (2005) C1303-C1311.

14. Mazzone, A., Tietz, P., Jefferson, J., Pagano, R. and LaRusso, N.F. Isolation and characterization of lipid microdomains from apical and basolateral plasma membranes of rat hepatocytes. **Hepatology** 43 (2006) 287-296.
15. Zheng, X. and Bollinger Bollag, W. Aquaporin 3 co-locates with phospholipase d2 in caveolin-rich membrane microdomains and is downregulated upon keratinocyte differentiation. **J. Invest. Dermatol.** 121 (2003) 1487-1495.
16. Guttman, J.A., Samji, F.N., Li, Y., Deng, W., Lin, A. and Finlay, B.B. Aquaporins contribute to diarrhoea caused by attaching and effacing bacterial pathogens. **Cell Microbiol.** 9 (2006) 131-141.
17. Le Roy, C. and Wrana, J.L. Clathrin- and non-clathrin-mediated endocytic regulation of cell signaling. **Nat. Rev. Mol. Cell. Biol.** 6 (2005) 112-126.
18. Gurcel, L., Abrami, L., Girardin, S., Tschopp, J. and van der Goot, F.G. Caspase-1 activation of lipid metabolic pathways in response to bacterial pore-forming toxins promotes cell survival. **Cell** 126 (2006) 1135-1145.
19. Padanilam, B.J. Cell death induced by acute renal injury: a perspective on the contributions of apoptosis and necrosis. **Am. J. Physiol. Renal. Physiol.** 284 (2003) F608-F627.
20. Szabo, C. Mechanisms of cell necrosis. **Crit. Care Med.** 33 (2005) S530-S534.
21. Broker, L.E., Kruyt, F.A. and Giaccone, G. Cell death independent of caspases: a review. **Clin. Cancer Res.** 11 (2005) 3155-3162.
22. Lang, F., Gulbins, E., Szabo, I., Lepple-Wienhues, A., Huber, S.M., Duranton, C., Lang, K.S., Lang, P.A. and Wieder, T. Cell volume and the regulation of apoptotic cell death. **J. Mol. Recognit.** 17 (2004) 473-480.
23. Bortner, C.D. and Cidlowski, J.A. A necessary role for cell shrinkage in apoptosis. **Biochem. Pharmacol.** 56 (1998) 1549-1559.
24. Bortner, C.D. and Cidlowski, J.A. The role of apoptotic volume decrease and ionic homeostasis in the activation and repression of apoptosis. **Pflugers Arch.** 448 (2004) 313-318.
25. Bortner, C.D. and Cidlowski, J.A. Apoptotic volume decrease and the incredible shrinking cell. **Cell Death Differ.** 9 (2002) 1307-1310.
26. Sidhaye, V., Hoffert, J.D. and King, L.S. cAMP regulation of AQP5: Distinct acute and chronic effects in lung epithelial cells. **J. Biol. Chem.** 280 (2004) 3590-3596.
27. Schmittgen, T.D., Zakrajsek, B.A., Mills, A.G., Gorn, V., Singer, M.J. and Reed, M.W. Quantitative reverse transcription-polymerase chain reaction to study mRNA decay: comparison of endpoint and real-time methods. **Anal. Biochem.** 285 (2000) 194-204.
28. Song, K.S., Li, S., Okamoto, T., Quilliam, L.A., Sargiacomo, M. and Lisanti, M.P. Co-purification and direct interaction of Ras with caveolin, an integral membrane protein of caveolae microdomains. Detergent-free purification of caveolae microdomains. **J. Biol. Chem.** 271 (1996) 9690-9697.
29. Jablonski, E.M., Webb, A.N., McConnell, N.A., Riley, M.C. and Hughes Jr. F.M. Plasma membrane aquaporin activity can affect the rate of apoptosis but is inhibited after apoptotic volume decrease. **Am. J. Phys.-Cell Phys.** 286 (2004) C975-C985.